Fourier-Transform Infrared Study of Azide Binding to the Fe_{a3}-Cu_B Binuclear Site of Bovine Heart Cytochrome *c* Oxidase: New Evidence for a Redox-Linked Conformational Change at the Binuclear Site†

Motonari Tsubaki* and Shinya Yoshikawa

Department of Life Science, Faculty of Science, Himeji Institute of Technology, Kanaji 1479-1, Kamigoori-cho, Akou-gun, Hyogo 678-12, Japan

Received June 10, 1992; Revised Manuscript Received October 6, 1992

ABSTRACT: Azide binding to the Fe_{a3}-Cu_B site of cytochrome *c* oxidase purified from bovine heart mitochondria was investigated in various redox levels by Fourier-transform infrared spectroscopy. In the fully oxidized state there were two azide species bound to the binuclear center, one (major) exhibiting an azide ($^{14}N_3$) antisymmetric stretching band at 2051 cm^{-1}, and the other (minor) at 2039.5 cm^{-1}. The former is considered to be in a bridging structure between Fe_{a3}^{3+} and Cu_B^{2+}, whereas in the latter species a bridging structure may not exist on the basis of the azide isotope substitution technique. Upon addition of cyanide to the preformed fully oxidized cytochrome *c* oxidase–azide complex, a new azide species exhibiting a sharp antisymmetric stretching band at 2032.5 cm^{-1} was formed. The cyanide is considered to be coordinated to the Cu_B^{2+} center (not observable by infrared spectroscopy), whereas the azide presumably still in a bridging structure. This cytochrome *c* oxidase–azide–cyanide ternary complex is relatively stable, and cyanide ion replaces the 2032.5-cm^{-1} azide species very slowly, resulting in the formation of the Fe_{a3}^{3+}–C–N–Cu_B^{2+} bridging structure characterized by the 2152-cm^{-1} band. Upon the introduction of 1 electron equivalent to the fully oxidized cytochrome *c* oxidase–azide complex, an azide band at 2003.5 cm^{-1} developed. Upon further introduction of electron equivalents, the 2003.5-cm^{-1} band disappeared and a new azide band at 2015.5 cm^{-1} appeared. In these partially reduced states azide coordinates to the Fe_{a3}^{3+} center presumably in an end-on fashion and cannot form a bridging structure any more. These observations are consistent with our proposal that two kinds of conformational changes can occur at the binuclear site on the basis of cyanide binding to the partially reduced cytochrome *c* oxidase; the first one occurs upon introduction of the first electron presumably to the Cu_B center, and the second one occurs upon introduction of the second or third electron presumably to the Fe_a or Cu_A center (Tsubaki & Yoshikawa, 1993; preceding paper in this issue).

A detailed Fourier-transform infrared (FT-IR)[1] study for cyanide binding to cytochrome *c* oxidase (CcO) has been described in the preceding paper in this issue (Tsubaki & Yoshikawa, 1993). In the fully oxidized resting state, it has been proposed that an unknown ligand (X) forms a bridging structure between heme a_3 and Cu_B (Fe_{a3}^{3+}–X–Cu_B^{2+}) on the basis of the presence of the antiferromagnetic interaction between these two metal centers (Barnes et al., 1991; Tweedle et al., 1978). We showed that when cyanide ion (CN^-) was added to the resting enzyme, an exchange of the bridging ligand from X to CN^- occurred, resulting in a formation of the bridging structure, Fe_{a3}^{3+}–C–N–Cu_B^{2+} (ν_{C-N} = 2152 cm^{-1}) (Tsubaki & Yoshikawa, 1993; preceding paper in this issue). However, upon the reduction of the Cu_B center the bridging structure is broken and the cyanide remains bound to the Fe_{a3}^{3+} center as Fe_{a3}^{3+}–CN^- (ν_{C-N} = 2132 cm^{-1}). Further reduction of the Fe_a and/or Cu_A centers seems necessary to cause the binding of cyanide to Cu_B^{1+} to produce the 2093-cm^{-1} band, indicating some stereochemical change around the Cu_B center (Tsubaki & Yoshikawa, 1993; preceding paper in this issue). Upon further reduction of the Fe_{a3} center, a second cyanide ion may bind to the Cu_B^{1+}–CN center, at a higher cyanide concentration, to give a new infrared band at 2037 cm^{-1}. The latter cyanide species seems to be oriented toward the Fe_{a3}^{2+} center. Therefore, in the fully reduced state the distance between the two metal centers is estimated to be even larger (Tsubaki & Yoshikawa, 1993; preceding paper in this issue).

Another specific inhibitor for the heme a_3–Cu_B site of CcO, having a potential efficiency as an infrared probe, is azide ion (N_3^-). However, in the past, the inhibitory mechanism of the azide ion upon CcO has not been understood well (Wilson, 1967; Wilson et al., 1972). Several electron paramagnetic resonance (EPR) studies (Goodman, 1984; Goodman & Leigh, 1987; Shaw et al., 1978; van Gelder & Beinert, 1969; van Gelder et al., 1967; Wilson et al., 1976; Wilson & Leigh, 1972) have revealed that upon partial reduction of CcO in the presence of azide ion two sets of EPR signals (g = 2.77, 2.18, 1.74, higher redox potential species, and g = 2.88, 2.19, 1.64, lower redox potential species) which are considered to be derived from heme a_3^{3+}–N_3^- developed subsequently in order (Goodman, 1984). These observations indicate that there is a redox-linked conformational change at the heme a_3–Cu_B binuclear site even for CcO–azide complex. (It is also not clear whether the azide ion can bind to the heme a_3^{3+}–Cu_B binuclear site in the fully oxidized state of CcO.) To obtain the detailed informations on the redox-linked conformational

---

† A part of this investigation was supported by Grants-in-Aid from the Ministry of Education, Culture and Science of Japan.

* To whom correspondence should be addressed, at the Department of Life Science, Faculty of Science, Himeji Institute of Technology, Kanaji 1479-1, Kamigoori-cho, Akou-gun, Hyogo 678-12, Japan.

[1] Abbreviations: FT-IR, Fourier-transform infrared; CcO, cytochrome *c* oxidase; EPR, electron paramagnetic resonance; 0/4 state, fully oxidized state; 1/4 state, 1 electron equivalent reduced state; 2/4 state, 2 electron equivalents reduced state, 3/4 state, 3 electron equivalents reduced state; 4/4 state, fully reduced state.

0006-2960/93/0432-174$04.00/0

change at the heme a_3–Cu_B binuclear site, it is highly necessary to reveal the nature of azide binding to the binuclear site by infrared spectroscopy. Several infrared studies for hemoproteins have been reported using azide ion as a probe, but those were only for hemoglobins and myoglobins (Alben & Fager, 1972; McCoy & Caughey, 1970). Very recently an infrared study of azide binding to CcO at five different redox levels has been reported (Yoshikawa & Caughey, 1992). They proposed that azide ion binds to Cu_B^{2+} as well as Fe_{a3}^{3+} in the partially reduced enzymes but not to Fe_{a3}^{3+} in the fully oxidized (Yoshikawa & Caughey, 1992).

In the present study we have performed a very accurate infrared difference spectroscopic measurements using a double-beam FT-IR spectrometer. By utilizing a new spectral deconvolution technique based on a least squares curve fitting approach (Tsubaki et al., 1992), we have analyzed overlapping azide stretching infrared bands and have been able to reveal the existence of two azide stretching bands bound to the CcO redox centers in the fully oxidized state. The existence of these two bands was confirmed independently in the spectrum at lower azide concentration, where practically no free azide ion exists. Ligand exchange upon addition of cyanide observed by continual FT-IR spectral measurements revealed the existence of another metastable azide intermediate species bound to the CcO redox centers in the fully oxidized state. Analyses of the overlapping azide stretching bands of the partially reduced CcO revealed an additional two bound azide species sensitive to the redox level of the metal centers as reported by Yoshikawa and Caughey (1992). The present results are, however, not fully compatible with the proposal of Yoshikawa and Caughey (1992). Present observations prompted us to propose that similar redox-linked conformational changes at the binuclear site with those observed in the CcO–CN complex (Tsubaki & Yoshikawa, 1993; preceding paper in this issue) are also operative, at a first approximation, when azide is bound to the binuclear site. Thus the observed redox-linked conformational changes at the binuclear site may be very important for a physiological turnover of the enzyme and may have a direct role for the oxygen reduction to water and the proton pumping mechanism.

MATERIALS AND METHODS

Preparation of CcO Sample. Cytochrome *c* oxidase (CcO) was isolated from bovine heart using the method of Yoshikawa et al. (1988) with some modifications as described in the preceding paper (Tsubaki & Yoshikawa, 1993).

Sodium azide solution (0.1–0.2 M) in the D_2O buffer was introduced with a Hamilton microsyringe to the concentrated CcO solution to convert the resting form of the enzyme to the azide-bound fully oxidized form (final azide concentration 0.3–2 mM; specified in the legends of figures). Sodium azide was obtained from Nacalai Tesque (Kyoto, Japan) for natural abundance $Na^{14}N_3$, from ICON (Mt. Marion, NY) for $Na^{15}N^{14}N^{14}N$ (99 atom % pure), and from Berlin Chemie (Berlin, FRG) for $Na^{15}N^{15}N^{14}N$ (95 atom % pure).

Neutralized potassium cyanide solution (0.2–0.5 M) in the D_2O buffer was introduced with a Hamilton microsyringe to the preformed CcO–N_3 solution to convert the azide-bound form of the enzyme to the cyanide-bound fully oxidized form. These manipulations were performed at 4 °C or on ice to retard the exchange reaction. This conversion could be monitored spectroscopically by the Soret band peak shift from around 421 to 428 nm as described previously for the addition of CN^- to the resting form of CcO (Tsubaki & Yoshikawa, 1993; preceding paper in this issue). The following potassium cyanide isotopes were used: $K^{12}C^{14}N$ (natural abundance, Nacalai Tesque); $K^{12}C^{15}N$ (99.4 atom % ^{15}N, Isotec Inc.); $K^{13}C^{14}N$ (99 atom % ^{13}C, Isotec Inc.); $K^{13}C^{15}N$ (99, 99 atom % ^{13}C, ^{15}N, Icon). Other chemicals used were the highest quality available and were used without further purification.

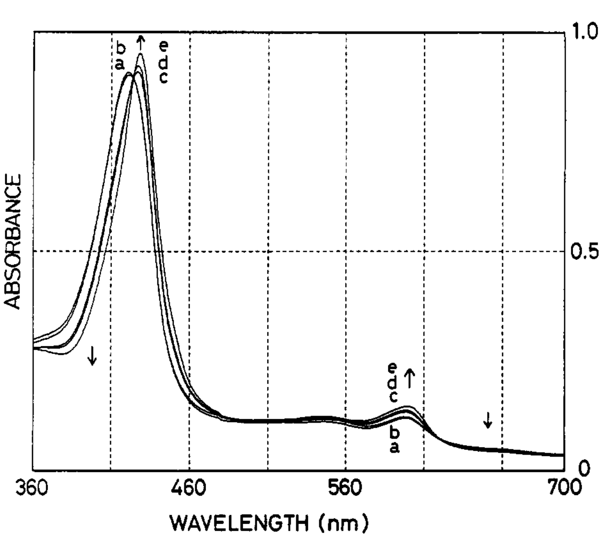

FIGURE 1: Visible absorption spectra of (a) the resting CcO (fully oxidized, 0/4 state), (b) CcO–$^{15}N^{14}N^{14}N$ complex in the fully oxidized state (0.3 mM azide concentration), and (c–e) the effect of addition of potassium cyanide ($^{12}C^{15}N$) (final concentration 1.2 mM) to the preformed azide complex in D_2O buffer. Temperature 25 °C.

The partially reduced oxidase preparations were obtained as follows (Yoshikawa & Caughey, 1982): the concentrated enzyme solution (typically 2 mM on heme A basis) in the H_2O buffer which had been mixed with sodium azide in a small glass tube sealed with a rubber septum was flushed for 1 h at room temperature with pure N_2 gas which had been moistened with a scrubbing bottles of pure water (H_2O or D_2O). Two syringe needles (one for inlet, the other for outlet) were attached to the rubber septum. The calculated amount of β-NADH solution was introduced to the deoxygenated enzyme solution through the rubber septum using an air-tight syringe, followed by further flushing with N_2 gas for 30 min. The sample solutions in the tube, phenazine methosulfate (2 mM) solution, and IR cells were then transferred into a glove box which had been purged with pure N_2 gas. The phenazine methosulfate solution (0.5 μL) was then introduced anaerobically to start the reduction of the redox centers. The sample solution was then introduced into the IR cell anaerobically using a disposable syringe.

Measurements of Fourier-Transform Infrared Spectra. Fourier-transform infrared (FT-IR) spectra were measured as described in the preceding paper (Tsubaki & Yoshikawa, 1993).

RESULTS

Effect of Addition of Sodium Azide on the Visible Absorption Spectra of Fully Oxidized CcO. Addition of sodium azide (final concentration from 0.2 up to 1.3 mM) to the fully oxidized CcO sample caused a small spectral change in the visible region, particularly a slight Soret peak shift from 421 to 420.5 nm (Figure 1; from line a to line b). This shift, although very small, was fully reproducible and could be seen more clearly as a development of absorption at 419 nm in the difference spectra (spectra not shown). This spectral change was very similar to the one previously reported by

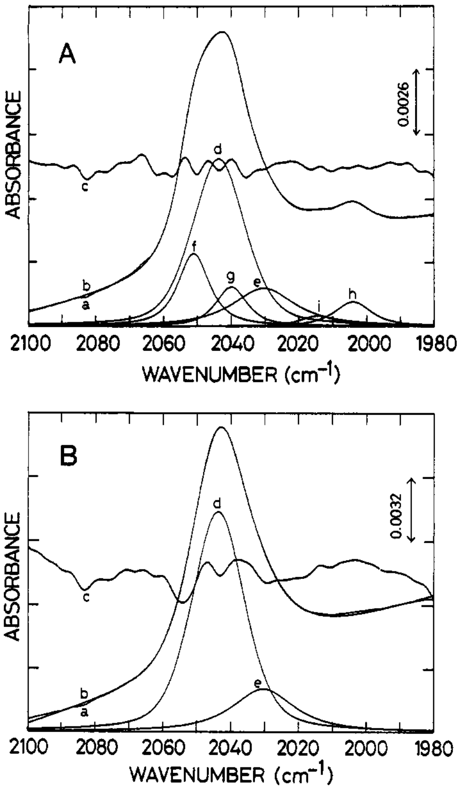

FIGURE 2: (A) FT-IR spectrum of fully-oxidized (0/4-state) CcO in the presence of azide ($^{14}N_3$, 1.3 mM) (a) and its deconvolution (d–h). Reconstituted spectrum b and difference spectrum c (ordinate is expanded by 10 times) are also included. (B) FT-IR spectrum of fully-reduced (4/4-state) CcO in the presence of azide ($^{14}N_3$, 1.3 mM) (a) and its deconvolution (d and e). Reconstituted spectrum (b) and difference spectrum (c) (ordinate is expanded by 10 times) are also included. The spectra were sums of 400 cycles of spectral accumulation (40 min accumulation) with the nominal spectral resolution at 4.0 cm^{-1}. Temperature, 10 °C.

Muijsers et al. (1971), confirming the binding to azide to the chromophore of the fully oxidized form of CcO.

Fully Oxidized State at Higher Azide Concentration Comparable with CcO Concentration. A typical infrared spectrum of the fully oxidized CcO (0/4 state) in the presence of 1.3 mM of sodium azide ($^{14}N_3$) is shown in the range from 2100 to 1980 cm^{-1} in Figure 2 (A, line a). In this region N=N=N antisymmetric stretching vibrations of free and bound azide ions are expected to appear. The inspection of the broad infrared band centered around 2043 cm^{-1} suggests that this band is composed of at least three components located around 2050, 2040, and 2005 cm^{-1}. The most intense one peaked around 2040 cm^{-1} is likely due to the free azide ion ($^{14}N_3$) in the buffer since free $^{14}N_3$ ion in the D_2O medium was reported to have its antisymmetric vibration at 2041 cm^{-1}. Indeed, in the H_2O buffer the infrared band corresponding to the 2043-cm^{-1} band shifted to higher frequency around 2047.5 cm^{-1} and overlapped with the 2051-cm^{-1} band (spectrum not shown).

Upon addition of sodium dithionite to the premixed CcO–azide ($^{14}N_3$) solution, the redox centers were reduced very rapidly and completely (resulting in 4/4 state) on the basis of the visible absorption spectroscopy. The infrared spectrum of this preparation is shown in Figure 2 (B, line a). Only one band centered at 2043.5 cm^{-1} was apparent, suggesting that, indeed, the 2043.5-cm^{-1} band in Figure 2A was due to the free azide ($^{14}N_3$) ion and that in the fully reduced state there was no bound azide to CcO (except the immobilized azide in the protein matrix of CcO; see below).

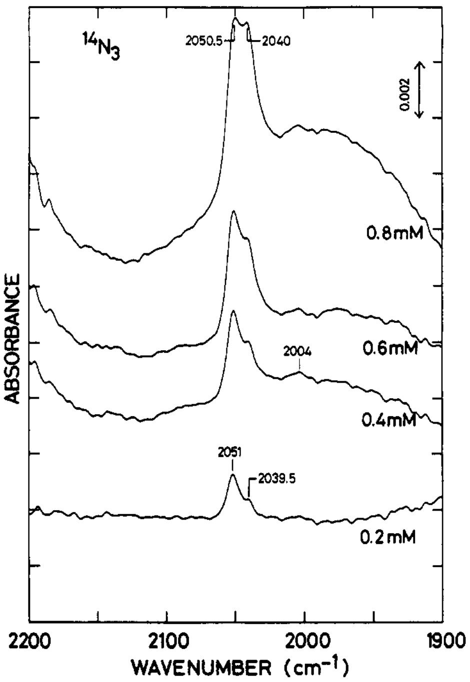

FIGURE 3: FT-IR spectra of fully-oxidized (0/4-state) CcO in the presence of various concentrations of $^{14}N_3$ (from 0.2 to 0.8 mM) in D_2O buffer. Other conditions were the same as in Figure 2.

To test this assumption, we tried to fit the infrared spectrum in Figure 2B using a linear combination of Gaussian and Lorentzian curves (Tsubaki et al., 1992). However, the fitting was not satisfactory; instead, it was found that two symmetrical bands at 2043.6 (line d) and 2030.4 cm^{-1} (line e) with 60% and 15% Gaussian character, respectively, were required to obtain a reasonable fitting (Figure 2B). The 2043.6-cm^{-1} band (line d) is apparently due to the free azide ion. The nature of the 2030.4-cm^{-1} band (line e) is not clear, but is most likely due to the immobilized azide ion in the protein matrix, other than the redox centers, of the CcO molecule. Assuming both of these bands present in the fully oxidized state in the presence of sodium azide, we tried to deconvolute the complex feature centered around 2043 cm^{-1} in Figure 2A. A total of 6 bands (d–i) including two bands observed in the fully reduced state (Figure 2B, lines d and e) were required to fit the spectrum satisfactorily (Figure 2A). Thus three infrared bands with medium intensities at 2050.8 (f), 2039.9 (g), and 2004.0 cm^{-1} (h) and a very weak band at 2013.6 cm^{-1} (i) are candidates for azide species bound to the redox metal centers of the enzyme.

Fully Oxidized State at Lower Azide Concentration. To obtain further insights into a mechanism of azide binding to the redox metal centers in the enzyme, the concentration of free azide had to be reduced since its infrared band at 2043.6 cm^{-1} obscured other overlapping bands. Decreasing of the azide ion concentration down to 0.4 mM resulted in no interference from free azide ion as shown in Figure 3. Three infrared bands at 2051, 2039.5, and 2004 cm^{-1} persisted and agreed with those obtained by the spectral deconvolution technique (f–h in Figure 2A). The frequencies of these bands were found to be independent of the azide concentration at least from 0.2 to 1.3 mM. Substitution of the buffer medium from D_2O to H_2O did not affect the frequencies of these three bands, and therefore, these bands are most likely due to the azide bound to the metal centers inside of the protein matrix of CcO.

The weak band at 2004 cm^{-1} and the small feature at 2014 cm^{-1} (line i) in Figure 2A were ascribed to the partially reduced

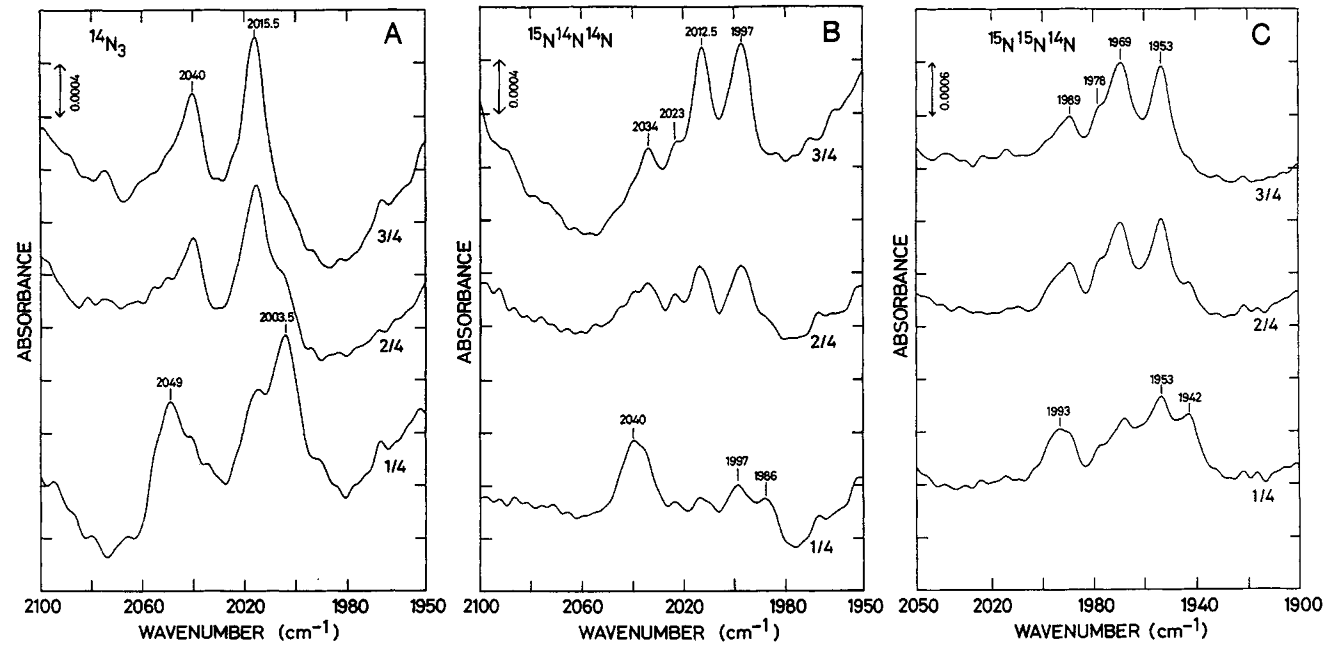

FIGURE 4: (A) FT-IR spectra of partially reduced (3/4, 2/4, and 1/4-state in descending order) CcO in the presence of $^{14}N_3$ (0.4 mM). (B) FT-IR spectra of partially reduced (3/4, 2/4, and 1/4-state in the descending order) CcO in the presence of $^{15}N^{14}N^{14}N$ (0.4 mM). (C) FT-IR spectra of partially reduced (3/4, 2/4, and 1/4-state in the descending order) CcO in the presence of $^{15}N^{15}N^{14}N$ (0.4 mM). All the spectra were measured in the H_2O buffer. Other conditions were the same as in Figure 2.

CcO–azide species as shown in the next section. Thus there are two azide species bound to the metal centers in the fully oxidized $^{14}N_3$ complex, i.e., the 2051- and 2039.5-cm^{-1} bands. It is apparent that the azide binding site giving the 2051-cm^{-1} band has a slightly higher affinity than the other giving the 2039.5-cm^{-1} band (Figure 2A and Figure 3).

A use of isotopic substitution is another powerful technique to analyze the overlapping infrared bands. In the case of azide ion, substitution of $^{14}N_3$ with terminally labeled $^{15}N^{14}N^{14}N$ (or $^{15}N^{15}N^{14}N$) made the interpretation of the overlapping bands more difficult due to the splittings of the azide antisymmetric stretching mode. However, it was obvious that there were at least three bands around 2039, 2035, and 2022 cm^{-1} for the $^{15}N^{14}N^{14}N$ complex as indicated by its asymmetric band shape of the major band (spectra not shown).

Partially Reduced States at Lower Azide Concentration. We further conducted spectral analyses on the partially reduced CcO samples at lower azide concentration (i.e., at 0.4 mM) to minimize the interference from free azide and the immobilized azide in the protein matrix. Figure 4 (A, B, and C) shows FT-IR spectra in 2100–1900-cm^{-1} region for the various partially reduced states (1/4, 2/4, and 3/4 states) of the $^{14}N_3$, $^{15}N^{14}N^{14}N$, and $^{15}N^{15}N^{14}N$ complexes, respectively. In the 1/4 state, there were two major infrared bands at 2049 and 2003.5 cm^{-1} for the $^{14}N_3$ complex (Figure 4 A, lower), three major bands at 2040, 1997, and 1986 cm^{-1} for the $^{15}N^{14}N^{14}N$ complex (Figure 4B, lower), and three major bands at 1993, 1953, and 1942 cm^{-1} for the $^{15}N^{15}N^{14}N$ complex (Figure 4C, lower), respectively. Spectral features in the 2/4 and 3/4 states were very similar to each other but different from those of the fully oxidized (0/4 state) and 1/4 states. In the 2/4 and 3/4 states there were two major bands at 2040 and 2015.5 cm^{-1} for the $^{14}N_3$ complex, whereas there were four bands at 2034, 2023, 2012.5, and 1997 cm^{-1} for the $^{15}N^{14}N^{14}N$ complex and at 1989, 1978, 1969, and 1953 cm^{-1} for the $^{15}N^{15}N^{14}N$ complex. Although these spectra in Figure 4 were measured in the H_2O buffer, there was not much difference from those in the D_2O buffer in terms of peak location nor band intensity (spectra not shown). On the basis of the closeness of the frequencies, the 2049- and 2040-cm^{-1} bands for the $^{14}N_3$ complex in the partially reduced states (corresponding bands for the $^{15}N^{14}N^{14}N$ complex are the 2040-cm^{-1} band and the split pair at 2034 and 2023 cm^{-1}, respectively) may be identical to, or very similar to, those in the fully oxidized state, i.e., the 2051- and 2039.5-cm^{-} bands for the $^{14}N_3$ complex. On the basis of this assumption, the complex feature in the spectrum of the $^{15}N^{14}N^{14}N$ complex in the fully oxidized state (Figure 3B) can be explained by the overlapping of the 2039-cm^{-1} band (major) and the split pair at 2034 and 2023 cm^{-1}. Very similar arguments can be made for the $^{15}N^{15}N^{14}N$ complex. Observed and tentative assignments of these azide infrared bands are summarized in Table I (for the justification of the assignments, see Discussion).

Effects of Addition of Cyanide Ion to the Preformed CcO–Azide Complex. Upon addition of potassium cyanide (final concentration 1.2 mM) to the preformed CcO–azide complex (at an azide concentration of 0.3 mM), the visible absorption spectrum changed quickly and drastically: the Soret band peak shifted from 420.5 to 426 nm, the α band became intensified, and a weak feature around 660 nm disappeared (Figure 1, from b to c). Longer storing of this sample at room temperature caused a further shift of the Soret band (to 428 nm) and the intensification of the α band (Figure 1, from c to e). At the final stage (Figure 1, spectrum e) the visible absorption spectrum could not be distinguished from that of the CcO–cyanide complex in the fully oxidized state, indicating that azide ions that had been bound to the redox centers of CcO were replaced completely with cyanide ions.

The time course studies on the ligand exchange reaction from azide ion to cyanide ion by FT-IR spectroscopy, however, revealed the presence of a relatively stable intermediate during the exchange reaction. In Figure 5, representative infrared spectra showing the ligand exchange reaction are presented. In the left two panels, bound $^{14}N_3$ (0.3 mM) was replaced with $^{13}C^{15}N$ (1.2 mM) in 24 h at 4 °C. At the very early stage of the reaction (within first 10 min after the addition of cyanide) there was a very sharp azide band at 2032.5 cm^{-1} together with weak features at 2053 and 2015.5 cm^{-1} (spectrum

Table I: Band Assignments of Azide Antisymmetric Stretching Vibrations Bound to the Fe_{a3}-Cu_B Binuclear Center of Cytochrome *c* Oxidase in Various Redox States

redox state	$^{14}N_3$	$^{15}N^{14}N^{14}N$	$^{15}N^{15}N^{14}N$	coordination structure (see Figure 6)	spin state (Fe_{a3}^{3+})
fully-oxidized (0/4 state)	2051	2039	1994	b	high
	2039.5	2034?	1989?	a	high
		2023?	1978?		
one-electron-reduced (1/4 state)	2049	2040	1993	b	high
	2040?	2034?	1989?	a?	high
		2023?	1978?		
	2015.5	2012.5?	1969?	e	low
		1997?	1953?		
	2003.5	1997	1953	d	low
		1986	1942		
two-electron-reduced (2/4 state)	2040	2034	1989	a	high
		2023	1978		
	2015.5	2012.5	1969	e	low
		1997	1953		
three-electron-reduced (3/4 state)	2040	2034	1989	a	high
		2023	1978		
	2015.5	2012.5	1969	e	low
		1997	1953		

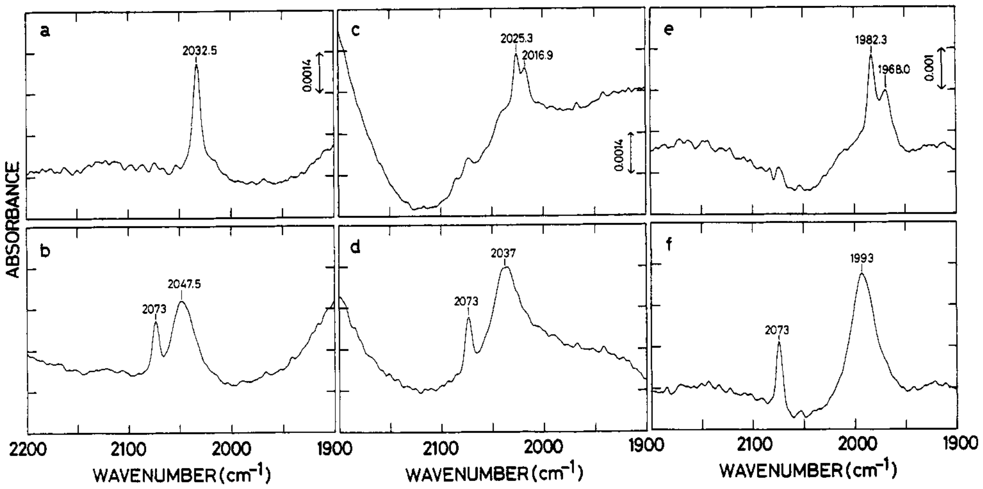

FIGURE 5: Effects of addition of cyanide ($^{13}C^{15}N$, 1.2 mM) to the preformed $^{14}N_3$–CcO complex ($^{14}N_3$ 0.4 mM) ((a) & (b)), to the preformed $^{15}N^{14}N^{14}N$–CcO complex ($^{15}N^{14}N^{14}N$, 0.4 mM) ((c) & (d)), and to the preformed $^{15}N^{15}N^{14}N$–CcO complex ($^{15}N^{15}N^{14}N$, 0.4 mM) ((e) & (f)). FT-IR spectra were recorded at (a) 40 min after, (b) 24 h after, (c) 40 min after, (d) 24 h after, (e) just after, and (f) 25 h after the addition of cyanide, respectively. Other conditions were the same as in Figure 2, except the temperature, 4 °C.

not shown). In the next stage (from 10 min after to 1 h after) there was only one sharp band persisting at 2032.5 cm^{-1}, and the weak features seen in the early spectrum had completely disappeared (Figure 5a). Then two infrared bands began to develop concomitantly at 2073 and 2047.5 cm^{-1}, and the sharp band at 2032.5 cm^{-1} became weaker and, in the final stage, it was gone completely (Figure 5b). The 2073-cm^{-1} band is due to the ^{13}C–^{15}N stretching vibration of the Fe_{a3}^{3+}–^{13}C–^{15}N–Cu_B^{2+} conformer of CcO as reported in the preceding paper (Tsubaki & Yoshikawa, 1993). The 2047.5-cm^{-1} band is due to free azide N=N=N antisymmetric stretching band in the H_2O medium.

Similar exchange reactions but using $^{15}N^{14}N^{14}N$ or $^{15}N^{15}N^{14}N$ and $^{13}C^{15}N$ were pursued by the same technique. At a very early stage of the reaction there were four infrared bands at 2041, 2025.3, 2016.9, and 1999.6 cm^{-1} for the $^{15}N^{14}N^{14}N$ complex (spectrum not shown). The two weak bands at 2041 and 1999.6 cm^{-1} seem to correspond to the 2053 and 2015.5 cm^{-1} bands, respectively, of the $^{14}N_3$ complex. Two major infrared bands at 2025.3 and 2016.9 cm^{-1} in the next stage (Figure 5c) may correspond to the 2032.5-cm^{-1} band of the $^{14}N_3$ complex (Figure 5a). The split 2025.3- and 2016.9-cm^{-1} bands were losing their intensity during the exchange reaction, and both bands were finally replaced with two infrared bands at 2073 and 2037 cm^{-1} (Figure 5d). The latter is due to free azide ion ($^{15}N^{14}N^{14}N$) in the H_2O medium. Very similar results were obtained for the $^{15}N^{15}N^{14}N$ complex as shown in Figure 5e and -f.

Neither the frequencies nor the band intensities of these intermediate bands (the 2032.5-cm^{-1} band in Figure 5a, the split 2025.3–2016.9-cm^{-1} bands in Figure 5c, and the split 1982.3–1968.0-cm^{-1} bands in Figure 5d) showed any change when the replacing ligand was changed from $^{13}C^{15}N$ to $^{12}C^{14}N$, $^{13}C^{14}N$, or $^{12}C^{15}N$ (spectra not shown). In addition, substitution of the H_2O buffer by the D_2O buffer did not affect these bands. Thus these bands appearing during the ligand exchange reactions can be assigned to the CcO-bound azide species and are not due to a bound cyanide mode nor a coupled mode of the bound azide and cyanide.

The nature of the weak features appearing in the very early stages of the exchange reaction is not clear in this study. The 2053-cm^{-1} band for the $^{14}N_3$ complex is most likely to be the unreacted 2051-cm^{-1} band of CcO in the fully oxidized state in the presence of $^{14}N_3$ (Figure 3). But we should not neglect the possibility that the 2053-cm^{-1} band is a short-lived intermediate in the early stages of the ligand exchange reaction

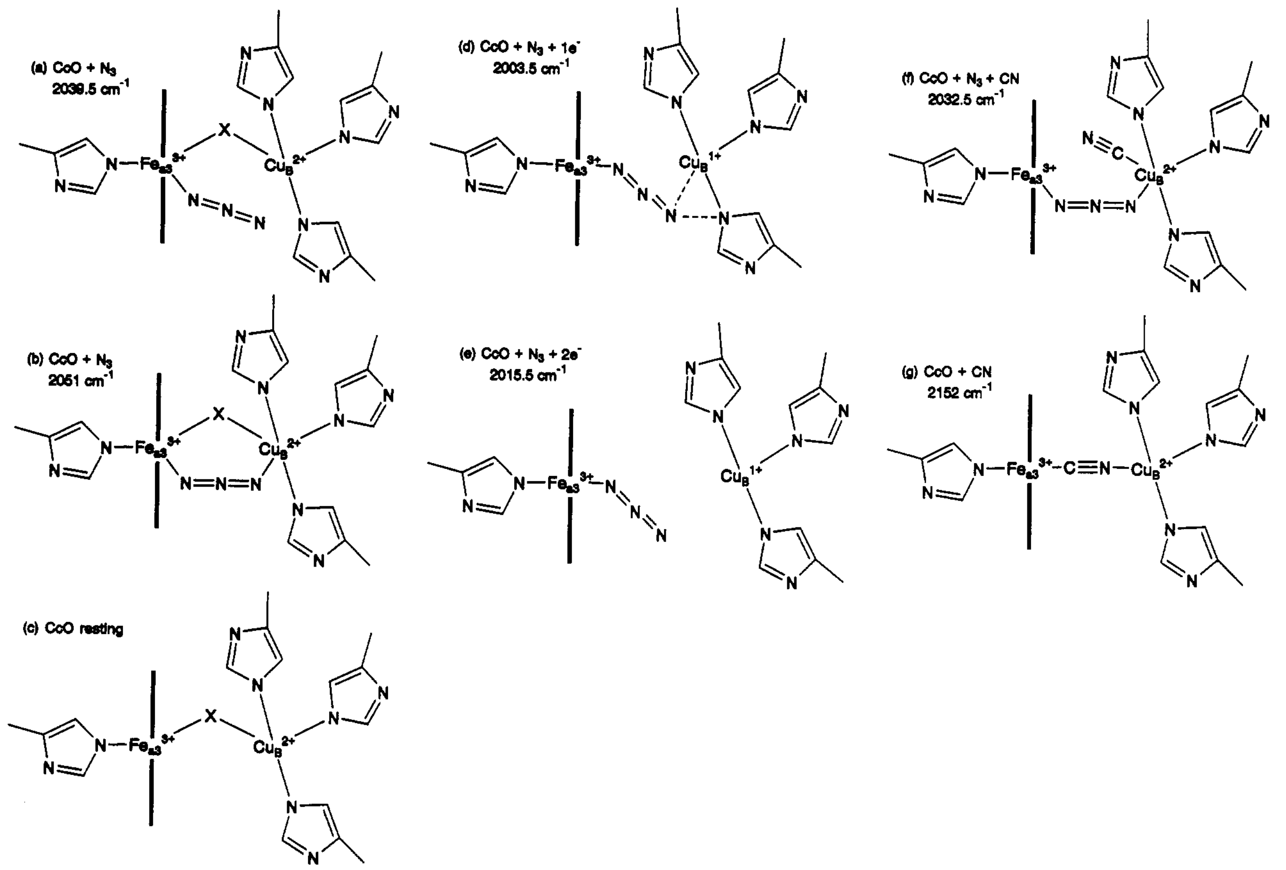

FIGURE 6: Proposed azide-binding models at the Fe_{a3}–Cu_B site of CcO in various redox levels and in the CcO–azide–cyanide ternary complex.

since this band was reproducibly 2–3 cm^{-1} higher in frequency than the 2051-cm^{-1} band in the repeated measurements.

DISCUSSION

Azide Binding to CcO in Various Redox States. Azide binds to metal centers in two ways, with covalent bonding and with ionic bonding. When the metal is ferric heme iron in hemoglobin (Hb) [or myoglobin (Mb)], it is known that bound azides give two azide antisymmetric stretching frequencies at 2047 (2045) and 2025 (2023) cm^{-1} in H_2O buffer (Alben & Fager, 1972). The former is derived from the covalently bound species and in a low-spin state, whereas the latter is from the species that bind to the ferric ion with an ionic interaction and, therefore, in a high-spin state. The bound azide vibrations from the fully oxidized CcO–azide complex showed two kinds of modes, the major band at 2051 and the minor band at 2039.5 cm^{-1}. Since both of these bands could be replaced with a minimum amount of cyanide [which gives the Fe_{a3}^{3+}–C–N–Cu_B^{2+} bridging structure characterized by the 2152-cm^{-1} band (Tsubaki & Yoshikawa, 1993; preceding paper of this issue)], the azide ion must occupy the same or overlapping site with this bridging cyanide, i.e., between the two metal centers. Therefore, the azide is presumably coordinated to the Fe_{a3}^{3+}–Cu_B^{2+} binuclear center with a terminal nitrogen atom. This view is consistent with the visible absorption spectral change (Figure 1).

Both of these bound azide vibrations seem to be derived from ferric high-spin state on the basis of their frequencies [horse heart Mb, 2045.8 cm^{-1}; sperm whale Mb, 2045.6 cm^{-1}; HbA, 2047 cm^{-1} (Alben & Fager, 1972; McCoy & Caughey, 1970; Tsubaki et al., 1981); heme B^{3+}–azide complex (5-coordinated), 2044 cm^{-1} (Caughey et al., 1977), Mn^{3+}Mb–azide complex, 2039 cm^{-1} (Yu & Tsubaki, 1980)]. The splitting of the $^{15}N^{14}N^{14}N$ antisymmetric modes for these high-spin azide species mentioned above were in the range from 11 to 12 cm^{-1} (Tsubaki and Yoshikawa, unpublished), whereas the separation of the 2039.5-cm^{-1} mode for the $^{15}N^{14}N^{14}N$ complex (2034 and 2023 cm^{-1}) was found to be exactly within this range. Thus the 2039.5-cm^{-1} band seems a typical ferric azide high-spin species and, therefore, the azide binding structure of the 2039.5-cm^{-1} species of the fully oxidized enzyme can be shown as in Figure 6a.

As an alternative possibility the 2039.5-cm^{-1} band could be a Cu_B^{2+}–N═N═N species as suggested by Yoshikawa and Caughey (1992). But this assignment seems inconsistent with the observation of this band even in the 3/4 state where the Cu_B center is expected to be almost fully reduced (Goodman, 1984).

On the other hand, the nature of the major azide species (2051-cm^{-1} band) is clearly different from those typical high-spin azide species nor low-spin species (that should appear in the region below 2025 cm^{-1}; see later). The 2051-cm^{-1} band did not show any detectable splitting upon replacement with $^{15}N^{14}N^{14}N$, indicating that the strength of the two internal N═N bonds of azide molecule was very similar to each other (Pate et al., 1986, 1989). The site that gave the 2051-cm^{-1} band was shown to have apparently higher azide-binding affinity than the site that gave the 2039.5-cm^{-1} band. This observation seems to rule out the possibility that the 2051-cm^{-1} band is due to the azide associated with the protein moiety near the binuclear site (Yoshikawa & Caughey, 1992). These observations together with the notion that azide molecule has electron orbitals available for the interaction with metal only at the terminal nitrogens strongly suggest that the 2051-cm^{-1} species is derived from the bridging azide between the two metal centers (Fe_{a3}^{3+}–N═N═N–Cu_B^{2+}) (Table I & Figure 6b).

In the fully oxidized state (0/4 state), addition of azide did not show any detectable change in the EPR spectra (Tsubaki and Hori, unpublished), confirming a previous observation (van Gelder & Beinert, 1969). Therefore, the 2051-cm^{-1} species (and possibly the 2039.5-cm^{-1} species as well) in the fully oxidized state the two paramagnetic metals (Fe_{a3}^{3+} and Cu_B^{2+}) are still forming a spin–spin coupled, EPR-undetectable, bimetallic center. Thus we assumed that an unknown shared bridging ligand, denoted as X, still exists for the 2051- and 2039.5-cm^{-1} species as shown in Figure 6a,b.

Upon partial reduction of the metal centers of CcO it has been speculated that the distance between the Fe_{a3} center and the Cu_B center increases. In the preceding paper we have shown that three kinds of such conformational change can occur on the basis of cyanide binding to the redox centers of CcO in the various redox states: the first one occurs upon introduction of the first electron presumably to the Cu_B center, and the second one occurs upon introduction of the second or the third electron presumably to the Fe_a or Cu_A center, whereas the third one occurs upon reduction of the Fe_{a3} center (Tsubaki & Yoshikawa, 1993). Our present observations on the azide binding to the binuclear center in the partially reduced state can be well understood on the basis of this scheme as follows.

The 2003.5-cm^{-1} species which appears only in the 1-electron equivalent reduced (1/4) state (where only the Cu_B center is in reduced state) is very similar to the low-spin heme B(Fe^{3+})–azide–pyridine complex (2004 cm^{-1}) (Caughey et al., 1977). It is very peculiar why in the 1-electron equivalent reduction of CcO caused such a large decrease of the antisymmetric stretching frequency. It is also strange that the separation of the peak frequencies of the split pair (1997 and 1986 cm^{-1}) for the $^{15}N^{14}N^{14}N$ complex is not so large compared to those of typical low-spin $^{15}N^{14}N^{14}N$ complexes (HbA, 16.5 cm^{-1}; horse heart Mb, 16.3 cm^{-1}; Tsubaki & Yoshikawa, unpublished). Caughey et al. (1977) proposed that the lowered frequency of the low-spin form of heme B(Fe^{3+})–azide–pyridine (2004 cm^{-1}) compared to those found in the low-spin form of Hb– and Mb–azide complexes (2025 cm^{-1}) is due to the absence of the interaction with distal histidine in the low-spin form of Hb– and Mb–azide complexes, whereas in the pyridine solution a significant interaction between pyridine and azide is expected. In this context the existence of a direct interaction between a histidine residue at the binuclear site and the bound azide in this partially reduced state may be essential (Figure 6d). However, this unusual azide antisymmetric vibration could be explained also by a direct charge effect of the Cu_B^{1+} center near the bound azide molecule.

The 2015.5-cm^{-1} species developed in the further reduced states (i.e., 2/4 and 3/4 reduced states) where the Fe_a and Cu_A centers, in addition to the Cu_B center, were reduced. Thus the distance between the Fe_{a3}^{3+} and the Cu_B^{1+} centers seems to become much larger, allowing the binding of azide to Fe_{a3}^{3+} in a typical low-spin state (Figure 6e). The observed large separation of the peak frequencies of the split pair (2012.5 and 1997 cm^{-1}) is almost the same as those of the typical low-spin $^{15}N^{14}N^{14}N$ complexes described before, supporting our proposal.

Relationship between Azide Infrared Bands and EPR Signals. Low-temperature (9–15 K) EPR spectroscopy of isolated CcO titrated potentiometrically in the presence of azide revealed the formation of two distinct species of low-spin Fe_{a3}^{3+}–azide complex that differ in redox properties and *g* values (Goodman, 1984). The EPR signal appearing at lower potential has principal *g* values of 2.88, 2.19, and 1.64; that appearing at higher potential has *g* values of 2.77, 2.18, and 1.74.

Thus it can be concluded that the Fe_{a3}^{3+}–$^{14}N_3$ species showing the 2003.5-cm^{-1} band (that appears only in the 1/4 state) is assignable to the one having the $g = 2.77$ signal, whereas the Fe_{a3}^{3+}–$^{14}N_3$ species showing the 2015.5-cm^{-1} band (that appears in the 2/4 and 3/4 states) is corresponding to the one having the $g = 2.88$ signal. We have postulated that in the 3/4 and 2/4 states the Cu_B center is fully-reduced (Table I) and the Fe_{a3}^{3+} and Cu_B^{1+} centers are well separated each other; thus the spin–spin coupling between the low-spin Fe_{a3}^{3+}–azide center and the Cu_B center is completely destroyed, and the typical low-spin Fe_{a3}^{3+}–azide EPR signal ($g = 2.88$) appears. In the 1/4 state most of the electron resides on the Cu_B center, and therefore, the spin–spin coupling is also absent. However, the distance of the binuclear center metals may not be so large that some interactions between the low-spin Fe_{a3}^{3+}–azide moiety and the Cu_B^{1+} center [or its His ligand(s)] still exist to produce the $g = 2.77$ signal. It should be stressed that among these two EPR species the species giving the $g = 2.77$ signal has not been found in the enzyme in the mitochondrial membrane preparation (Wilson et al., 1976; Wilson & Leigh, 1972) and is considered to be specific for the isolated enzyme. This fact indicates that this kind of intermediate species (i.e., the $g = 2.77$ species and, therefore, the 2003.5-cm^{-1} species) at the binuclear site may be not populated in a significant amount during the physiological turnover of CcO enzyme in the mitochondrial membrane.

Simultaneous Binding of Azide and Cyanide to the Binuclear Center in the Fully Oxidized State. The nature of the metastable 2032.5-cm^{-1} band formed upon addition of cyanide to the preformed fully oxidized CcO–$^{14}N_3$ complex is enigmatic. It is of great interest to note that there was no infrared band assignable to the CcO-bound cyanide mode in the early stage of the exchange reaction (i.e., Figure 5a,c,e). It is unlikely that cyanide works only by triggering the reaction and exists as a free state in the neighborhood of the active site when the bound azide ion exists as the 2032.5-cm^{-1} species. Rather, we consider that cyanide is presumably bound to the Cu_B^{2+} center simultaneously, forming a CcO–azide–cyanide ternary complex when the 2032.5-cm^{-1} band is formed. However, this Cu_B^{2+}–C–N moiety cannot be detected by infrared spectroscopy, presumably due to its intrinsic weaker extinction coefficient compared to that of Cu_B^{1+}–C–N.

The azide-binding structure to the binuclear center of the CcO–azide–cyanide ternary complex is also not clear. At first glance, the split features at 2025.3–2016.9 cm^{-1} and at 1982.3–1968.0 cm^{-1} for the $^{15}N^{14}N^{14}N$– and the $^{15}N^{15}N^{14}N$–cyanide ternary complexes (Figure 5c,e), respectively, seem to indicate the nonequivalence of the two N=N internal stretching force constants of the bound azide in an end-on fashion, caused by a breakage of the bridging structure or by a weakening of the bond between the terminal nitrogen of bridging azide and the Cu_B^{2+} center upon the cyanide binding to the Cu_B^{2+} center. However, there are two difficulties in accepting this explanation. First, the infrared intensities of the split bands are not equivalent each other (those with higher frequencies are stronger than the others). If the splittings were due to the nonequivalence of the two N=N internal stretching force constants, the intensities of the two split bands should be almost identical to each other as shown in Figure 4B,C. Second, the frequency separation between the split bands are anomalous: 8.4 cm^{-1} for the $^{15}N^{14}N^{14}N$–cyanide ternary complex and 14.3 cm^{-1} for the $^{15}N^{15}N^{14}N$–cyanide ternary complex. The splittings should be much closer to each other for these two complexes (see Figure 4B,C and Table I). These two observations seem to suggest that the splittings are not due to the nonequivalence of the two N=N internal stretching force constants of the bound azide but due to the vibrational coupling (i.e., Fermi resonance)[2] of the azide antisymmetric stretching mode and an unknown infrared inactive mode at the binuclear center. If this was the case, there should be only one azide antisymmetric mode before the vibrational coupling for the $^{15}N^{14}N^{14}N$– or $^{15}N^{15}N^{14}N$–cyanide ternary complex, indicating that the azide must be in a bridging structure between the Fe_{a3}^{3+} and the Cu_B^{2+} centers in the ternary complexes. Thus we assumed this "Fe_{a3}^{3+}–azide–Cu_B^{2+}–cyanide complex" as shown in Figure 6f.

On the proposed ternary complex scheme, interesting observations had been reported by van Buuren et al. (1972) and Chan and co-workers (Brudvig et al., 1980; Stevens et al., 1979). In the former report, van Buuren et al. (1972) observed that the addition of azide accelerated sharply the binding of cyanide to the fully oxidized enzyme and, during this reaction, the binding of azide seemed to precede the reaction with cyanide on the basis of visible absorption spectroscopy. They proposed a conformational change accompanying the azide binding to CcO that facilitated the subsequent initial weak binding of cyanide. Their working model may be understood more clearly by our present assumption: The direct replacement of the unknown bridging ligand (X) between Fe_{a3}^{3+} and Cu_B^{2+} with cyanide may be a very slow process. However, azide ion can coordinate to Fe_{a3}^{3+} and Cu_B^{2+} due to its binding geometry even in the presence of bridging ligand (X) (Figure 6a), and the binding causes the weakening of the bond strength of the bridging ligand (X) and facilitates the subsequent cyanide binding to Cu_B^{2+} as shown in Figure 6f. This cyanide or another cyanide ion may eventually replace the bridging azide, resulting in the formation of the Fe_{a3}^{3+}–C–N–Cu_B^{2+} species (the 2152-cm^{-1} species) as shown in Figure 6g.

On the other hand, Chan and co-workers (Brudvig et al., 1980; Stevens et al., 1979) observed that the addition of azide together with nitric oxide (NO) to the fully oxidized enzyme resulted in a reduction of the Fe_{a3}^{3+} center, followed by the binding of NO to the Fe_{a3}^{2+} center to form a "triplet complex" on the basis of EPR spectroscopy. A possible reaction scheme at the binuclear site, "$Fe_{a3}^{3+} + N_3^- + NO \rightarrow Fe_{a3}^{2+} + N_2O + N_2$", was proposed and was verified by the observation of the production of N_2O by mass spectroscopy. Boelens et al. (1984) confirmed the observations above and proposed a similar reaction scheme:

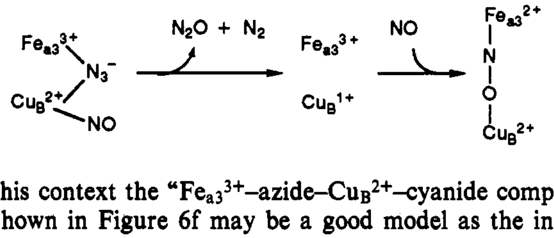

In this context the "Fe_{a3}^{3+}–azide–Cu_B^{2+}–cyanide complex" as shown in Figure 6f may be a good model as the initial intermediate of the reaction to form the "triplet complex".

The spin state of the iron in the "Fe_{a3}^{3+}–azide–Cu_B^{2+}–cyanide complex" is not clear at this stage, since the frequency of the 2032.5-cm^{-1} band for the $^{14}N_3$–cyanide–ternary complex is intermediate between high- and low-spin states. The location of the Soret band peak at 426 nm (Figure 1, spectrum c) suggests that the Fe_{a3}^{3+} center is in the low-spin state. We have tried to characterize this metastable species by EPR spectroscopy (X-band, 4.2 K; Tsubaki and Hori, unpublished), but no apparent indication of the presence of this new species could be observed, indicating that this species is also in a spin–spin coupled EPR-invisible state. This fact is consistent with the presence of the bridging azide with which the spin–spin coupling between Fe_{a3}^{3+} and Cu_B^{2+} is mediated.

It must be stressed again that this 2032.5-cm^{-1} azide species is replaced slowly, presumably with the Cu_B^{2+}-bound cyanide, resulting in a formation of the bridging structure (Fe_{a3}^{3+}–C–N–Cu_B^{2+}) (Figure 6g) to give the 2152-cm^{-1} band for $^{12}C^{14}N$ and 2073-cm^{-1} band for $^{13}C^{15}N$. It is also worthwhile to note that both the bridging azide species (2051-cm^{-1} band) and the terminally bound azide species (2039.5-cm^{-1} band) seem to be converted to the same 2032.5-cm^{-1} species and, finally, to the cyanide bridging structure. All these observations seem to suggest that the distance between the Fe_{a3}^{3+} and the Cu_B^{2+} centers is not so much different among the azide-bridged species (the 2051- and 2032.5-cm^{-1} species) (Figure 6a,f), the terminally bound azide species (the 2039.5-cm^{-1} species) (Figure 6b), and the cyanide-bridged species (the 2152-cm^{-1} species) (Figure 6g).

Implication to the Physiological Redox-Linked Conformational Change at the Binuclear Site. The site where dioxygen molecule is reduced to water by utilizing 4 electrons from reduced cytochrome *c* is the Fe_{a3}–Cu_B binuclear center. It has been believed that Cu_B is the primary electron acceptor of the binuclear site and that direct electron transfer between Fe_a and Fe_{a3} does not occur at physiological velocities. Consequently, the first two electrons to reduce bound dioxygen (O_2) must be donated from Fe_{a3}^{2+} and Cu_B^{1+}, yielding a peroxy intermediate (compound C). The formation of the compound C (peroxide complex) is thought to be followed by transfer of the third electron from Fe_a to Fe_{a3} via Cu_B. This causes breakage of the O–O bond and protonation of the product (oxygen atom), resulting in a formation of a tetravalent iron (ferryl)–oxo intermediate and a water molecule that remains coordinated to the Cu_B^{2+} center. Then the fourth electron is transferred, presumably from Fe_a to Cu_B followed by the reduction of Fe_{a3}^{4+} to Fe_{a3}^{3+} and the production of a second water (Chan & Li, 1990; Malmström, 1990).

However, the reason to believe that Cu_B is always the primary electron acceptor to the binuclear site seems not so strong. Rather we should consider the possibility that the structural modulation at the redox centers may retard the electron transfer from Cu_B to Fe_{a3} for the last two (or three) steps without allowing the direct electron transfer from Fe_a to Fe_{a3}. This scheme may explain the unexpected stabilities of the oxygenated form, Fe_{a3}^{2+}–O_2 (compound A), and its two-electron-reduced, (hydro)peroxide complex, Fe_{a3}^{3+}–OOH (compound C), allowing the direct identification of these compounds by resonance Raman spectroscopy (Ogura et al., 1990, 1991; Han et al., 1990a–d; Varotsis et al., 1989, 1990; Varotsis & Babcock, 1990). According to their results, the Cu_B center that is generally considered to be located at the very vicinity of the Fe_{a3} center lacks an apparent effect on the frequencies of the Fe_{a3}^{2+}–O_2, or the Fe_{a3}^{3+}–OOH compared to the corresponding species formed in other usual hemoproteins. Traditionally, the Cu_B center has been considered

---

[2] A similar vibrational coupling seems to occur in a met azide hemocyanin system also. EXAFS and electronic absorption data for met azide hemocyanin allow only a μ-1,3 bridging geometry of azide ion between two copper atoms, while resonance Raman data showed the splitting of the azide antisymmetric vibration upon $^{15}N^{14}N^{14}N$ substitution (Pate et al., 1986). Although Pate et al. (1986) ascribed this observation to the nonequivalence in bonding within the azide molecule due to a strong interaction with residue(s) in the protein pocket, a possibility raised in the present study should be considered.

to be an effective electron donor to the Fe_{a3}^{2+}-bound dioxygen or to the bound intermediates, and therefore, the binuclear site has been always treated as a unit; i.e., the Fe_{a3} and Cu_{B} centers were thought to be an inseparable binuclear site. These resonance Raman data were apparently inconsistent with this view. These two centers seem to behave more independently than we have tended to think previously, although the interaction between these two centers is still overwhelming compared to those between other combinations of the redox centers.

The electron donations from the Cu_{B} center seem to occur at the last two steps of the four electron-transfer reactions to dioxygen without allowing the direct electron transfer from Fe_a to Fe_{a3}. This mechanism is compatible with the proposal that these last two steps are linked to the proton pumping activity of CcO (Wikström, 1989). If the electron donations for the last two steps occurred exclusively from the Cu_{B} center, the understanding of the redox-linked conformational change(s) at the Cu_{B} center will be, apparently, a key point to reveal the mechanism of the proton pumping by this enzyme [Babcock & Wikström, 1992; see, however, Larsen et al. (1992)]. In this context, the CcO–azide complex in the partially reduced state, like the $\mathrm{Fe}_{a3}^{3+}\text{–N}{=}\text{N}{=}\text{N}\ \mathrm{Cu}_{\mathrm{B}}^{1+}/\mathrm{Fe}_a^{2+}$ state, has an important meaning. The highest occupied orbitals of azide are a set of degenerate nonbonding Π orbitals analogous to the set of degenerate Π^* in peroxide (Pate et al., 1989); thus this kind of azide complex may be a good model for understanding the catalysis of a postulated peroxide intermediate $\mathrm{Fe}_{a3}^{3+}\text{–O}^-\text{–O}^-\ \mathrm{Cu}_{\mathrm{B}}^{1+}/\mathrm{Fe}_a^{2+}$.

ACKNOWLEDGMENT

We thank Dr. Hiroshi Hori of Osaka University and Dr. Tatsushi Mogi of the University of Tokyo for helpful comments and discussions.

REFERENCES

Alben, J. O., & Fager, L. Y. (1972) *Biochemistry 11*, 842–847.

Babcock, G. T., & Wikström, M. (1992) *Nature 356*, 301–309.

Barnes, Z. K., Babcock, G. T., & Dye, J. L. (1991) *Biochemistry 30*, 7597–7603.

Boelens, R., Rademaker, H., Wever, R., & van Gelder, B. F. (1984) *Biochim. Biophys. Acta 765*, 196–209.

Brudvig, G. W., Stevens, T. H., & Chan, S. I. (1980) *Biochemistry 19*, 5275–5285.

Caughey, W. S., Maxwell, J. C., Thomas, J. M., O'Keeffe, D. H., & Wallace, W. J. (1977) in *Metal-Ligand Interactions in Organic Chemistry and Biochemistry* (Pullman, B., & Goldblum, N., Eds.) pp 131–152, D. Reidel Publishing Co., Dordrecht Holland.

Chan, S. I., & Li, P. M. (1990) *Biochemistry 29*, 1–12.

Goodman, G. (1984) *J. Biol. Chem. 259*, 15094–15099.

Goodman, G., & Leigh, J. S., Jr. (1987) *Biochim. Biophys. Acta 890*, 360–367.

Han, S., Ching, Y., & Rousseau, D. L. (1990a) *Proc. Natl. Acad. Sci. U.S.A. 87*, 8408–8412.

Han, S., Ching, Y., & Rousseau, D. L. (1990b) *Biochemistry 29*, 1380–1384.

Han, S., Ching, Y., & Rousseau, D. L. (1990c) *Proc. Natl. Acad. Sci. U.S.A. 87*, 2491–2496.

Han, S., Ching, Y., & Rousseau, D. L. (1990d) *J. Am. Chem. Soc. 112*, 9445–9451.

Larsen, R. W., Pan, L.-P., Musser, S. M., Li, Z., & Chan, S. I. (1992) *Proc. Natl. Acad. Sci. U.S.A. 89*, 723–727.

Malmström, B. G. (1990) *Chem. Rev. 90*, 1247–1260.

McCoy, S., & Caughey, W. S. (1970) *Biochemistry 9*, 2387–2393.

Muijsers, A. O., Tiesjema, R. H., & van Gelder, B. F. (1971) *Biochim. Biophys. Acta 234*, 481–492.

Ogura, T., Takahashi, S., Shinzawa-Itoh, K., Yoshikawa, S., & Kitagawa, T. (1990) *J. Biol. Chem. 265*, 14721–14723.

Ogura, T., Takahashi, S., Shinzawa-Itoh, K., Yoshikawa, S., & Kitagawa, T. (1991) *Bull. Chem. Soc. Jpn. 64*, 2901–2907.

Pate, J. E., Thamann, T. J., & Solomon, E. I. (1986) *Spectrochim. Acta 42A*, 313–318.

Pate, J. E., Ross, P. K., Thamann, T. J., Reed, C. A., Karlin, K. D., Sorrell, T. N., & Solomon, E. I. (1989) *J. Am. Chem. Soc. 111*, 5198–5209.

Shaw, R. W., Hansen, R. E., & Beinert, H. (1978) *Biochim. Biophys. Acta 504*, 187–199.

Stevens, T. H., Brudvig, G. W., Bocian, D. F., & Chan, S. I. (1979) *Proc. Natl. Acad. Sci. U.S.A. 76*, 3320–3324.

Tsubaki, M., & Yoshikawa, S. (1993) *Biochemistry* (preceding paper in this issue).

Tsubaki, M., Srivastava, R. B., & Yu, N.-T. (1981) *Biochemistry 20*, 946–952.

Tsubaki, M., Shinzawa-Itoh, K., & Yoshikawa, S. (1992) *Biophys. J.* (in press).

Tweedle, M. F., Wilson, L. J., García-Iñiguez, L., Babcock, G. T., & Palmer, G. (1978) *J. Biol. Chem. 253*, 8065–8071.

van Buuren, K. J. H., Nicholls, P., & van Gelder, B. F. (1972) *Biochim. Biophys. Acta 256*, 258–276.

van Gelder, B. F., & Beinert, H. (1969) *Biochim. Biophys. Acta 189*, 1–24.

van Gelder, B. F., Orme-Johnson, W. H., Hansen, R. E., & Beinert, H. (1967) *Proc. Natl. Acad. Sci. U.S.A. 58*, 1073–1079.

Varotsis, C., & Babcock, G. T. (1990) *Biochemistry 29*, 7357–7362.

Varotsis, C., Woodruff, W. H., & Babcock, G. T. (1989) *J. Am. Chem. Soc. 111*, 6439–6440.

Varotsis, C., Woodruff, W. H., & Babcock, G. T. (1990) *J. Biol. Chem. 265*, 11131–11136.

Wikström, M. (1989) *Nature 338*, 776–778.

Wilson, D. F. (1967) *Biochim. Biophys. Acta 131*, 431–440.

Wilson, D. F., & Leigh, J. S., Jr. (1972) *Arch. Biochem. Biophys. 150*, 154–163.

Wilson, D. F., Lindsay, J. G., & Brocklehurst, E. S. (1972) *Biochim. Biophys. Acta 256*, 277–286.

Wilson, D. F., Ereciñska, M., & Owen, C. S. (1976) *Arch. Biochem. Biophys. 175*, 160–172.

Yoshikawa, S., & Caughey, W. S. (1982) *J. Biol. Chem. 257*, 412–420.

Yoshikawa, S., & Caughey, W. S. (1992) *J. Biol. Chem. 267*, 9757–9766.

Yoshikawa, S., Tera, T., Takahashi, Y., Tsukihara, T., & Caughey, W. S. (1988) *Proc. Natl. Acad. Sci. U.S.A. 85*, 1354–1358.

Yu, N.-T., & Tsubaki, M. (1980) *Biochemistry 19*, 4647–4653.